NISTIR 6768

A Predictive Ionization Cross Section Model for Inorganic Molecules

J. W. Hastie

NIST
National Institute of Standards and Technology
Technology Administration, U.S. Department of Commerce

NISTIR 6768

A Predictive Ionization Cross Section Model for Inorganic Molecules

J.W. Hastie,
Ceramics Division

MSEL

July 2001

U.S. Department of Commerce
Donald L. Evans, Secretary

National Institute of Standards and Technology
Karen H. Brown, Acting Director

A Predictive Ionization Cross Section Model for Inorganic Molecules

J. W. Hastie
National Institute of Standards and Technology
Gaithersburg, MD 20899, U.S.A.

Abstract

To address a long-standing lack of experimental data for electron impact ionization cross sections for inorganic molecules, or the availability of a reliable predictive method, we have developed a modified classical model. The model relies on the known or expected ionic bonding character of most inorganic and, particularly, of high temperature molecules. Based on isoelectronic analogy, use is made of available cross section data for the elements, together with known or readily calculated ionization potentials for the molecules of interest. Very good agreement is found for several of the species considered here and elsewhere using the more extensive and primarily ab initio binary-encounter Bethe model. Good overall agreement is also found with experimental results for fifty-one species, with up to ten constituent atoms. The model appears to be at least as accurate as experimental methods, is free of adjustable parameters, and is generally applicable to inorganic and high temperature molecules. An expected relationship with polarizability is found in addition to support for a concept involving additivity of ionic cross sections. Model result implications for the accuracy of thermochemical data in existing databases are considered.

Keywords: ionization, cross section, high temperature, models, thermochemical data, autoionization.

1. Introduction

Electron impact ionization cross sections (σ) are important in diverse areas of science and technology. They are, and have been for nearly half a decade, particularly pertinent in the application of high temperature mass spectrometry to thermodynamic studies, as has recently been discussed in detail elsewhere [1]. In many instances, measurement of σ's for high temperature molecules is either impractical or inaccurate. For studies reliant upon estimates of molecular ionization cross sections, the estimates are based on additivity (or some empirical reduction thereof) of the component atomic cross sections. The additivity approximation has its basis in studies on organic or covalently bonded species. On the other hand, the majority of high temperature species are characterized by ionic bonding, where electron transfer to the more electronegative atom leads to anion-cation association with characteristic strong coulombic interaction. Ionic models have proven very satisfactory for prediction of bond dissociation energies [2] and of ionization potentials [3]. Here, we examine the application of an ionic model to the prediction of ionization cross sections. The cross sections considered here, and those of greatest utility, are for electron impact production of singly charged positive ions, including parent and all fragment ions. As multiply charged ions are usually negligible at the energies of interest (~10 – 50 eV), these σ's are effectively total ionization cross

sections. From theoretical and practicality-of-application considerations, emphasis is given here to σ_m , the maximum ionization cross section at energy E_m. These σ_m values can then be scaled, although with reduced accuracy, to other values of E.

Classical, molecular-orbital-based models have recently been applied, with some success, to a few relatively low molecular weight inorganic species such as SiF and SiF_2 [4]. However, the extension of such molecular-orbital-based models to high molecular weight, many electron high temperature species is problematic.

The difference in electron configurations, underlying cross section behavior, between an atom and its cation or anion can be considerable. It appears likely, therefore, that use of atomic cross-section-based models may be unreliable and hence lead to larger than expected errors in derived thermochemical or similar species-concentration-related properties. The importance of σ's and their uncertainty estimates have been noted in standard thermodynamic databases [5, 6]. In the present study, we show that these earlier error assignments to σ's can, in some instances, be greatly underestimated.

2. Approach

2.1 Model basis

Various classical models (discussed below) have been developed earlier, relating σ_i for orbital i with E, B_i , N_i , where E is the electron impact energy, B_i the orbital energy, and N_i the orbital electron occupation number (see literature summary in [1]). In one of these models, explicit consideration of orbital radii is also made [7]. These models have been applied with reasonable success primarily to the elements and secondarily to gaseous, covalently bonded molecules. While such models have a theoretical basis, empirical scaling has generally been required to obtain agreement with experiment, particularly for molecules. Also, complex molecular orbital calculations have been required to obtain model input values of B_i and N_i , in addition to other parameters.

We consider here the development of a predictive σ model, requiring minimal a priori knowledge (ie. ionization potential) of the molecule of interest and with a single gobal scaling factor, obtained from an averaged small set of experimental values. For high temperature species, the model must account for their characteristic ionic (vs covalent) bonding. Cross sections for high temperature species are usually associated with mass spectrometry experiments [1], where the ionization potential, B, is readily measured or can be calculated from an ionic model [3]. However, higher-level orbital energies are generally not known. From appearance potential studies, E_m , the energy at which σ is at a maximum, is often found to be much lower than for covalent species, particularly for open-shell electron configurations. For such cases, B, the energy of the lowest occupied molecular orbital, will have a dominant effect on the cross section.

Thus in its simplest and most practical form we consider the function (fn.) where:

$$\sigma_m \sim \text{fn. } (B, N, E_m) .$$

Hereafter, σ_m is taken to be at its maximum value and is designated as σ. Thus, for the present purposes, the energy scale is fixed at E_m. From consideration of the more detailed classical models discussed below, the form of the above σ relationship is suggested as:

$$\sigma \sim f N'/B, \qquad (1)$$

where f is a constant between like species (eg. atoms) and N′ is an empirical term we designate as an effective number of ionizable electrons. As will be shown (section 2.1.5), an explicit consideration of the functional dependence of N′ on E_m and B_i is unnecessary. Moreover, N′ is not necessarily an integer and is related very indirectly to the N term of classical models discussed below (sections 2.1.1, 2.1.2, 2.1.3). We stress here that the purpose of considering eq. (1) in this form is to relate σ's, at E_m , among various species categories, ie. atoms or molecules. Consideration of σ at other values of E is made separately (see section 3.6) where the energy dependence of N′ is explicitly considered. For discussion purposes, we designate the model described by eq. (1) as a modified classical method (MCM).

2.1.1. Binary-encounter Bethe (BEB) model simplification.

The BEB model [4] can be represented in the form:

$$\sigma_i \sim (N_i / B_i) (E + U_i + B_i)^{-1} (C),$$

for each contributing orbital i, and where
$C = 0.5 \ln x (1 - x^{-2}) + 1 - x^{-1} - \ln x (x + 1)^{-1}$,
$x = E / B_i$, and U_i is orbital kinetic energy.
Then $\sigma = \Sigma \sigma_i$. Values of B_i and U_i are obtained from Hartree-Fock molecular orbital calculations. For the lowest energy orbital, the experimental vertical ionization potential B is used. The terms within the collision factor C become more significant at higher E and particularly at $E > E_m$.

For high temperature and inorganic molecules, where we designate $E = E_m$ as the principal energy of interest, values of x are generally in the range, $x = 3 - 7$. Values of $E + B$ typically fall in the range $20 - 70$ eV. For the relatively low E's of the present application, we neglect U. It appears that the semiempirical form of the present model adequately accounts for this U term in an indirect manner. If the U term was significant and was not effectively compensated for, the model σ's would be expected to exceed the experimental values, but no such systematic trend is found. For these conditions, it can be shown that the product of the E-containing bracketed terms of the σ_i equation is, to a good approximation, constant for the above range of x, ie. well within the model and experimental σ uncertainties. Also, the empirical nature of N′ (discussed in section 2.1.5) is expected to account for differences between molecules in the E-containing terms. Thus, at E_m , the BEB model simplifies to the form of the present model, as given in equation (1). For relatively large values of x, such as would occur with closed shell multiatomic species, eg. SiF_4, WF_6, and W_2O_6, one might expect the approximations

made here to be less reliable. However, for such cases, the MCM model gives σ's in good agreement with experiment.

2.1.2 Mann (modified Bethe) model simplification.

The model approach of Mann [7], which applies exceptionally well to those elements where direct ionization is the main pathway, has the form:

$$\sigma_i = N_i \langle r \rangle^2 [E^{-1} \ln (E / B_i)]$$

where $\langle r \rangle^2$ are orbital (i) mean square radii. In practice, Hartree-Fock molecular orbital calculations are used to obtain $\langle r \rangle^2$ and B_i (higher level) data. The absolute $\sigma = \Sigma\sigma_i$ values are scaled using a single experimental value (ie. $\sigma_{Ar} = 2.83 \times 10^{-20} m^2$).

Empirically, we find for the non-gaseous elements that $\langle r \rangle^2 \sim B^{-1}$ and hence the Mann model and the present MCM model reduce to a similar form, for our conditions, where the bracketed term is constant to a good approximation. Similar arguments apply to a more recent version of this model (see [7]).

2.1.3 Gryzinski-binary encounter model simplification.

The Gryzinski model [8] has a similar form to that of the more recent BEB model, although in the latter case the E^{-1} term was replaced by $(E + U + B)^{-1}$. For our conditions (see section 2.1.1), collision terms involving x and the term E^{-1} simplify to an approximate constant, as was the case for the BEB model expression. The Gryzinski model, at E_m , then reduces to the form of eq. (1). Thus earlier classical and more current comprehensive models each may be simplified to the form of the present model. It should be noted, however, that our application of the complete form of the Gryzinski model to molecules of the type considered here did not lead to satisfactory results. A similar situation occurs for atoms, as indicated in [1].

2.1.4 Model dependences on E and B.

We note that for some molecular species, denoted MX, where $B_{MX} \sim d_{MX}^{-1}$ (the internuclear distance), the simplified Mann formula would indicate a higher order dependence of σ_{MX} on B_{MX}. Similarly, there exists a suggested relationship between σ and B^{-2} known as Thompson's Rule [9]. While the conditions leading to such a dependence are not typical of those for the species and conditions of interest here, we nevertheless carried out model tests for the relationship:

$$\sigma \sim N'/B^2 ,$$

and found much poorer accord with experiment. Also, very poor accord was found with Thompson's Rule, even for isoelectronic pair comparisons. Similarly, no empirical basis was found for possible model explicit inclusion of E^{-1} or E^{-2} terms which could be significant at high E_m values.

At this time we conclude that further refinements to the model are unwarranted, considering the model approximations and the present degree of uncertainty associated with atomic and, more particularly, molecular ionization cross sections.

2.1.5 Evaluation of N′ for MCM ionic model application.

In principle, we could assign N′ as the number of valence electrons in the highest occupied molecular orbital (HOMO) with an energy corresponding to B. For molecular species MX, knowledge of the electron distribution is needed for this purpose. Most of the species of interest can be considered ionically, as opposed to covalently, bonded; eg. M^+X^-. An ionic bonding model model has previously proven effective in predicting bond dissociation energies and ionization potentials, as mentioned earlier (section 1).

For each M^+, X^-, there exists an isoelectronic element M', X' with the same electron configuration and in some instances (particularly for X′) with similar size and, we assert, with similar cross section behavior. For M^+ and X^-, the ionic radii are close to the radii of M' and X' respectively. For higher valent M^{n+} cases, the M' radii are significantly larger [10]. Also, internuclear separations in ionic bonding molecules are significantly less than the combined M′ + X′ atomic radii. The proposed comparability between M^+ and M', for example, should be contrasted with the dramatic differences in $\sigma_M{}^+$ (free ion) and σ_M ,
eg. $\sigma_{Ba}{}^+ \sim 2 \times 10^{-20} m^2$ [11] vs. $\sigma_{Ba} \sim 17 \times 10^{-20} m^2$ [7]. (From this point on the $10^{-20} m^2$ unit factor will not be cited explicitly.) Such differences underscore the historical difficulties associated with atomic additivity cross section models.

As a key approximation to the MCM model, we obtain effective values for N' from M' and/or X' as follows. From the basic model form of eq. (1), it follows that:

$$N' = g\, \sigma_{M'}\, B_{M'}\,, \qquad (2)$$

and similarly for X'. Thus N' becomes an empirical parameter and is not necessarily an integer. The proportionality constant g is obtained by use of a value, or averaged species set of values, of, for instance, $\sigma_{M'}$ and $B_{M'}$ with an assigned value (s) of N′ based on the known atomic electron configurations and energies. For this purpose, we may select a case (s) where at E_m for M' only the HOMO level is ionizable, eg. Ca where N′ = 2. This calibration process is not essential, as a further empirical normalization for obtaining f (for molecules using eq. (1)) also encompasses g. However, this interim step provides useful model insight as we find a set of N' values for M', X' atoms that are consistent with expected valences and their periodicity. It is anticipated that the effect of many of the model simplifications made with respect to more rigorous models will be compensated for by this isoelectronic approach to model parameterization.

Combining eqs. (1) and (2), together with the model assumption that N'_{MX} is given by the sum of the N′ values for each M′ and X′, the molecular model is then given by:

$$\sigma_{MX} = k\, B_{MX}^{-1} (\sigma_M' B_M' + \sigma_X' B_X') , \qquad (3)$$

where k (= fg) is a fixed universal constant for all MX and other ionic bonding species. Corresponding expressions follow for the more polyatomic cases, ie. the prime terms continue to be summed for each additional atom. We note that the summation of N′ terms assumption has a parallel in the classical model (s) summation of orbital σ_i's. Also, the representation of N'_{MX} as σ - containing terms for isoelectronic atoms has the effect of introducing, empirically, collision factor information to the model, as discussed in section 2.1.1.

A value of k is obtained empirically from the slope of a linear least-squares fit to several reference species experimental σ_{MX} values versus the term following k in the above eq. (3). In principle, only a single experimental value is needed for this purpose. However, we averaged over several of the species where good experimental and model reliability was expected, ie. CsCl, CsI, SiO, and SiF_2, and where different laboratories and methods were used. With this approach, we find k = 0.62 (± 0.04). The species σ's for this reference set also fall within the 95% confidence limit for the complete (51 species) data set, as given later in section 3, Table 1, Fig. 1.

From the model expression (eq. 3), we see that the model form is that of a scaled additivity of isoelectronic atoms where the empirical factor (0.62) scales for the lower σ of moleceules versus atoms. The B ratios scale for the effect of molecule formation on the ionization level. Factors contributing to a σ reduction on molecule formation include: electron participation in bonding orbitals, formation of ion pairs with reduced orbital extension in space, and possible shielding of a normally accessible orbital by the presence of neighbor atoms or, more particularly, ions.

2.2 Model extension to an ion cross section additivity principle

An alternate, heuristically attractive form of the model is given by:

$$\sigma_{MX} = 0.62\, \sigma_M'(B_M'/B_{MX}) + 0.62\, \sigma_X' (B_X'/B_{MX}) ,$$

which may be considered an isoelectronic component, scaled ion-additivity model. The factor 0.62 accounts for the typical (though not necessarily universal) lowering of cross sections on molecule formation, while the B ratio terms also account for changes resulting from molecule formation. This form may also be considered as an ion additivity model, in contrast with conventional atom additivity models. Moreover, we typically find

$$B_M'/B_{MX} < 1 \text{ and } B_X'/B_{MX} \sim 2.$$

These factors then effectively account for the coulombic interaction-based expected inequalities $\sigma_X^- > \sigma_X'$ and $\sigma_M^+ < \sigma_M'$.

From the ionic model of ionization potentials [3], it follows that values of B_{MX} also include the coulombic effect of the presence of an adjacent, oppositely charged ion on the ease of electron removal during ionization. In the event that the model did not adequately represent the cross section differences between isolated M^+ vs. M' and X^- vs. X', we would expect to find systematic and opposite differences between model and experimental values for M' or X' dominance. No such trends have been found. We note that differences between σ_M^+ and $\sigma_{M'}$ can be small, eg. as for:
$C^{2+} \sim Be$, $Li^+ \sim He$, $K^+ \sim Ar$ (11).

From these considerations, it is possible to derive from the model or from experimental σ_{MX} data, values of σ_M^+, σ_X^-, etc. for additivity use, ie. where:

$$\sigma_{MX} = \sigma_M^+ + \sigma_X^-.$$

These ionic cross sections are then not those of isolated ions but are effective values for use as components of molecular species. A comprehensive set of ionic cross sections has been calculated, and the values generally follow the relations:

$$\sigma_X^-/\sigma_{X'} \sim 0.9\ (\pm 0.3)$$
$$\sigma_X^{2-}/\sigma_{X'} \sim 1.8\ (\pm 0.3);$$
for closed-shell configuration:
$$\sigma_M^+/\sigma_{M'} \sim 0.03\ (\pm 0.03)$$
$$\sigma_M^{2+}/\sigma_{M'} \sim 0.03\ (\pm 0.03);$$
for open-shell configuration:
$$\sigma_M^{n+}/\sigma_{M'} \sim 0.3 - 0.9 \text{ range.}$$

Here, the terms closed- or open- shell configuration have their usual meaning. That is, a closed-shell cation or anion molecular component has a full-shell electron complement, similar to that of a rare gas atom. The inherent stability of a closed-shell leads to relatively high B values and low σ values. Conversely, for the open-shell case, one or more electrons are readily available for ionization, leading to low B, high σ values.

While this ion-additivity approach is very satisfactory, we prefer the more rigorous model of eq. (3) where explicit inclusion of B_{MX} is considered. For cases where such data are not available or easily calculated, the ionic additivity form of the model may be useful.

2.3 Electron localization

2.3.1 Heteronuclear systems

For application of the model, consideration of electron localization is desirable, although it is not critical to the general applicability of the model, as the relative contribution of cation or anion centers to the nature of the ejected electron is generally accounted for by the $\sigma_M' B_M'$ (ie. N_M') and $\sigma_X' B_X'$ (ie. N_X') terms in eq. (3). For a cation closed-shell electron configuration, the cation contribution to the overall cross section is negligible, as noted in section 2.2. In addition, electron removal from a cation is appreciably more difficult than from a neutral isoelectronic atom. Hence, for such a case, the $\sigma_M' B_M'$ term is not included in eq. (3). For the open-shell case, both cation and anion contributions are considered.

In the extreme delocalization case we consider the bonding as covalent and we find, as in earlier studies [1], that

$$\sigma_{MX} \sim \sigma_M + \sigma_X .$$

For several of the systems considered here we find, from differences in electronegativity, from changes in binding energy on ionization, and from other bonding considerations, a comparable weighting of ionic and covalent character. In these cases, an average of the fully ionic and fully covalent models gives very good agreement with experiment (as will be shown in section 3.1).

Arguments concerning electron localization (ie. at M^+ or X^-, or both) may also be given support where ion intensity ($\sim \sigma$) vs. E appearance potential curves are known. For instance, the SiF, SiF_2, SiF_3 set of species is exceptionally well characterized from the σ vs. E measurements of Freund et al [12 – 14] and from the molecular orbital (MO) and BEB σ calculations of Kim et al [4]. For SiF, the σ vs. E curve is very similar to that of the M′ element Al. For SiF_2, the curve is shifted to higher E than for the M′ = Mg curve, consistent with an expected additional contribution of F^- to σ. A similar behavior is noted for SiF_3. These indirect arguments are verifiable, in this particular species set, from the MO results [4], where: for SiF about 90% of the orbital contributions to σ_M are of Si^+ character; for SiF_2, 70%; and for SiF_3, 25%.

In the MCM model, where the terms $\sigma_M' B_M'$ etc. derive from the concept of effective N′ contributions, the relative values of these terms for M′ and X′ are also indicative of orbital contributions to σ. Using this approach, we find 77% Si^+ character for SiF, 65% for SiF_2, and 25% for SiF_3, in good accord with the above MO results. Thus for these cation open-shell species, the inclusion of cation and anion terms in the model (eq. (3)) is consistent with independent MO results.

Application of the ionization potential ionic model to expected ionic bonded species, such as CsI and ZrO, gives good agreement with experimental B's, where electron loss is from the anion and primarily the cation, respectively. For significantly covalent species, such as GaCl, markedly different B values are obtained using an ionic model as compared with experiment. For GaCl, the ionic model yields B ~ 12 eV for

either anion or cation electron localization cases, versus 10.1 eV by experiment. Similar differences are found for SnCl.

Earlier theoretical work on diatomic metal halides indicated a predominantly ionic bonding-type [3, 17], and the location of the lowest removal energy (HOMO) electron and its B value were readily calculated. From the change in bonding energy resulting from ionization, as represented by $D_{MX}^{+} - D_{MX}$, the nature of the ejected electron could also be surmised [15]:

$$D_{MX}^{+} - D_{MX} = B_{MX} - B_{M} . \qquad (4)$$

Application of the MCM ionization cross section model to similar species utilizes an a priori assignment of the electron localization, similar to that of the earlier above-mentioned work.

For closed-shell species, such as the alkali halides, where the $M^{+}X^{-}$ configuration leads to $M^{+}X$ on ionization and $D_{MX}^{+} << D_{MX}$, the removed electron originates primarily at X^{-}. The rare gas atom, isoelectronic with X^{-}, is then used to represent the cross section properties of X^{-} which, in combination with the experimental B_{MX}, effectively accounts for the influence of M^{+} on the X^{-} electron removal energy. Similar arguments apply to other closed-shell, electron complement molecular species, eg. the dioxides of Ti, Zr, Ce, Th; and oxides such as BaO, Li_2O, UO_3 and W_2O_6, in addition to WF_6. For the heavier and more polyatomic of these species, ie. W_2O_6 and WF_6, we can expect a more delocalized electron character and the values of $D_{MXn}^{+} - D_{MXn}$ generally reflect this behavior. Thus for these latter cases, all nuclei are considered in the σ model calculation.

For open-shell molecular species, typically those where M is at less than its maximum valence, the most accessible electron is located at M^{n+}, eg. for the monoxides of V, Si, Ti, Zr, Hf, Y, Ce, La, Th, and U. In these cases (except for SiO), there is no significant difference between D_{MX}^{+} and D_{MX} and therefore M′ (M^{2+}) together with X′(O^{2-}) are used to model σ.

For sulfides and the other chalcogenides, which characteristically are more covalent than the corresponding oxides, the $D_{MS}^{+} - D_{MS}$ values indicate removal of a partly-bonding electron. Hence, for these (open-shell) species, S^{2-} (and Se^{2-}, Te^{2-}) and M^{2+} each contribute significantly to the ionized electron, eg. for US, GdS and PbS.

For very polyatomic cases, an increased delocalization in electron character results, eg. for As_4O_6 where M′ (Zn) and X′ (Ne) each contribute to σ. Similarly, for smaller species where a significant covalent character is present as evidenced by MO electron distributions, electronegativity differences, etc., a delocalized electron case applies, eg. for GaCl, GeCl, and SnCl. For GaCl, ionization greatly diminishes the bond energy, which is not in keeping with an ionic model and electron (e)-removal primarily from Ga^{+} which has two readily available e's. This observation further supports the other indicators of a significant covalency for this species, thereby leading to a low MCM

model σ value based on a Ga^+Cl^- charge distribution. These arguments are also supported by earlier molecular orbital results on charge distribution and orbital mixing [17]. For a partially covalent closed-shell species such as HCl, where e-removal for an ionic model would be from Cl^-, a large bond energy reduction would result from ionization, ie. similar to that of the alkali halides. However, only a small change is noted, in keeping with a delocalized electron character and significant covalency.

In principle, one can use electronegativity, molecular orbital calculations, or other bonding arguments, to estimate the degree of covalency or partial charge present in M^+X^- species, for instance. When this is done, eg. for GaCl, GeCl, SnCl, then a weighted averaging of σ's from the present ionic model and from additivity (~covalent case) can be shown to give much closer agreement with experiment (see section 3.1). For most high temperature species, the degree of ionicity is sufficiently large that such an adjustment is unnecessary.

2.3.2 Homonuclear systems

Homonuclear molecules M_n, typically where n = 2 – 5, are prevalent high temperature species. Here, the ionic model would not appear to be applicable. However, the principle of isoelectronic analogy may be successfully applied using the following formalism. For the simplest case of M_2, we represent the electron configuration as an electron pair bond, ie. M: : M, irrespective of the normal valence of M. Here, each M provides an electron pair to bond formation and each M nucleus formally becomes M^{2+} in the M_2 molecule. The isoelectronic M′ for M^{2+} is then used to model σ in the same manner as for heteronuclear species. Comparison between model and experimental σ's indicates this approach to be very reliable, as will be shown in section 3.2. Trimers and tetramers are modeled similarly.

2.4 Heteronuclear dimer systems

Dimers such as $(M_nX_m)_2$ where n, m ≥ 1 are particularly common high temperature species. From limited experimental evidence, the following empirical relationship has been developed [20] and is widely used [5]:

$$\sigma\,(MX)_2 = 1.5\,\sigma_{MX}\,.$$

In a more recent relationship, the 1.5 factor is reduced to 1.25 ± 0.35 [1]. Homonuclear systems have similarly been estimated and the reliability of such estimates will be indicated in section 3.4.

A model test of this dimer/monomer relationship can be made using the system

$$2\,WO_3 = (WO_3)_2.$$

An experimental value of σ = 11.4 is known for $(WO_3)_2$ [1]. As no σ value is available for WO_3, we use the ionic model to indicate a value of σ = 6.5. Similarly, the MCM model value for $(WO_3)_2$ is σ = 13.4. Application of the empirical 1.5 factor to the

monomer gives $\sigma = 9.8$ for the dimer. Each of these values is within the uncertainties of model and experiment. On the other hand, application of the atomic additivity model gives $\sigma = 26.2$.

2.5 Cross sections for the atoms

Experimental σ's are unavailable for a majority of atoms [1] and for some of the elements, where multiple studies have been carried out, appreciable differences have been noted. The only complete, self-consistent set of σ's appears to be the calculated results of Mann [7], which we have used for this work with a few noted exceptions. Comparison between Mann's values and experimental results, where available, is usually satisfactory with the notable exception of the Group IIIA elements measured by Freund et al [16]. The experimental values appear anomalously high (by ~ 37%), but Kim and Stone [21] have shown theoretically that autoionization has enhanced σ, as discussed below (section 2.5.1). Also, for Group IVA, the σ values of [16] are moderately higher (~20%) than those of [7]. Hence the experimental values [16] are used for Groups IIIA and IVA. For Group IA, the experimental σ_m values of Rb [18] and Cs [1] are also higher (~18%) than those of [7], on account of autoionization, and they are used in the model. For heavy elements such as Th, the abundance of energy levels increases the possibility of autoionization [19]. However, only direct ionization model σ values are available [7]. In summary, the following σ values, given in parentheses, were used here in preference to those of Mann [7]: Al (9.9), Ga (9.2), In (12.2), Rb (10.2), Cs (est. 13.1), Si (6.7), Ge (7.5), Sn (9.8), Pb (8.3), P (5.3), As (6.1), Sb (8.3). For the lightest elements H and He, more recent, accurate experimental and model results [1] supplant the Mann values.

We prefer Mann's values using his relation V as opposed to IV (see in [7]), the former being the basis for his later values [7]. In addition to the maximum values of σ and E, Mann's calculations also provide σ's as a function of E. These data, however, are only available in the recent survey [1]. It should be noted that if Mann's [7] data are renormalized to a more recent and more precise value of σ_{Ar} [16], they are decreased by 8%. This change is compensated for in the present work within the k normalization factor of eq. (3).

2.5.1 Autoionization-enhanced cross sections for the elements

In addition to direct ionization, which can be satisfactorily modeled [7, 22], a few elements are known or suspected to be candidates for excitation autoionization. This phenomenon can occur where excitation is to a quasi-bound state above the ionization level with decay to the ion state outweighing radiative decay [23]. Such an effect is expected to be limited to a relatively few elements where appropriate energy levels are present above, but near, the ionization limit.

In view of the periodicity of the electron configurations for the elements, candidate groups of elements can be, or have been, identified. These include, in decreasing order of significance, the groups III_A , I_A , and III_B. Relatively small cross section enhancements may be expected in a few other elements of groups IV_A, VI_B, and possibly the actinides. The best examples, established experimentally [16] and theoretically [21], are Al, Ga, and In, in addition to B and probably Tl [21]. As an aside, early experimental evidence for an unusually high σ_{Ga} was cited by Mann [7] from the work of K. Gingerich. The measurements of Freund et al [16] and the model values of Mann [7] are in good agreement for direct ionization cases; we have therefore selected the Freund et al values [16] for autoionization to supplement the Mann set [7] of atomic cross sections for use with the MCM σ model. When this is done, good model agreement is found for MX cases where M′ is an autoionized atom, consistent with the presence of a similar autoionization contribution to σ_{MX}.

2.6 Energy scaling of cross sections

In its most convenient and accurate form, the model provides maximum σ values (σ_m). Also, the majority of high temperature mass spectrometric cross sections available for comparison with the model are for E_m , or for some other single E value which is scalable to E_m. When scaling σ_m to other E values giving σ_E , any of the following five procedures may be used. Several of these procedures take into consideration the ionic bonding character of MX species. We estimate that E-scaling over a wide interval (ΔE) from E_m to values near B_{MX} , or vice versa, could lead to a doubling of the σ uncertainty (see section 3).

A number of scaling procedures are considered here as each has particular advantages/disadvantages. As noted elsewhere [1], methods based on a simple proportionality of σ and (E – B) are likely to be more uncertain over large ΔE, or where autoionization is present. For scaling over relatively large ΔE, the approach defined by eq. (8) is found to be more reliable than those of eqs. (5) – (7), but here E_m needs to be known. However, even when E_m is estimated, eq. (8) usually leads to more reliable σ's than eq. (7), for instance. In some cases, estimation of E_m can be problematic. The corresponding values for M′ (or X′ or both) appear to provide an upper limit estimate for E_m. We note that so systematic trends for predicting E_m are found for E_m/B ratios for MX species or between MX and M′ or X′. For closed-shell configurations, σ varies slowly over a large ΔE range near E_m and hence the accuracy of an E_m estimate is not critical to the σ-scaling result in this case.

In view of the additional σ_E uncertainty resulting from scaling from E_m to E values near the ionization threshold, it would seem desirable to carry out mass spectrometric experiments at E_m when utilizing the MCM model. This is often not practical, however, owing to interference from electron impact fragmentation, as discussed in detail elsewhere [1]. In principle, this difficulty can be largely avoided

through use of beam modulation [24]. A proper accounting of all fragment ions arising from the molecule of interest is also required when the mass spectrometric data are interpreted using model σ's which are total ionization cross sections for singly charged positive ions.

2.6.1 σ_E from σ_m and appearance potential curves

Actual values of E_m can usually be obtained most accurately from experimental appearance potential (AP), ie. ion intensity (I) vs. E curves. Relative values of σ_E / σ_m can also be obtained from such curves and these data may be used, together with model σ_m values, to obtain absolute values of σ_E. Thus $\sigma_E = \sigma_m (I_E/I_m)$. However, for cases where AP data are not available, the form of σ vs. E, up to E_m, may be approximated as that of M′ or X′ or some combination thereof, depending on the electron localization mode used in the model. This approach appears to be a reasonable approximation. For instance, the form of the σ_{Cd} vs. E curve [1] provides a good representation of the known curve for SnCl [25]. This approach is considered most suitable for cases when the electron is principally localized at either M or X.

2.6.2 σ_E from MCM model and (E – B) differences

The common practice of σ - scaling using (E – B) differences may be used although significant errors can occur [26, 27], particularly over large intervals or where autoionization is present. The assumption of the model concerning E/B terms terms in the BEB and other classical models also may be less reliable at higher E's (see section 2.1). Thus the model is likely to be most reliable for relatively low E_m cases (< 50 eV). Fortunately, many high temperature species are candidates for relatively low E_m behavior.

The following procedure is recommended, combining the MCM model with the common scaling approximation for $E < E_m$, namely: $\sigma_E \alpha (E - B)^{1.1} \alpha (E - B)$. Hence, to a good approximation:

$$\sigma_{MX,E} = 0.62 (\sigma_{M',E} B_{M'}) B_{MX}^{-1} (E - B_{MX})(E - B_{M'})^{-1} \quad , \qquad (5)$$

and similarly for X′ electron localization. Good agreement is found, for instance, with the experimental σ(E) data for SiF [12] and SiF_2 [13].

2.6.3 σ_E from $\sigma_{M'}$ and (E – B) differences

Alternatively, the following scaling procedure may be used to convert σ_{MX} to a value at $E < E_m$; eg. for X′ electron localization:

$$\sigma_{MX,E} = \sigma_{M',E} \, \sigma_{MX} \, \sigma_{X'}^{-1} \, (E - B_{MX}) \, (E - B_{X'})^{-1}. \qquad (6)$$

A term in $(E_{M',max} - B_{M'}) / E_{MX,max} - B_{MX})$, not included in this relation, can be assumed to be near unity to a good approximation, thereby avoiding use of E_m values which may not be well known.

2.6.4 σ_E from σ_{MX} and (E – B) differences

It should be noted that a few cases may occur, eg. for X′ a rare gas, where $E < B_{X'}$. For such a case, the procedure of eq. (6) is not applicable and E_m must be considered explicitly and is either measured or approximated by $E_{m,M'(or\,X')}$. Then

$$\sigma_{MX,E} = \sigma_{MX} \ (E_{MX} - B_{MX}) \ (E_{m,MX} - B_{MX})^{-1} \ . \qquad (7)$$

A more rigorous analytical model, based on a coupling of classical limiting behavior at low (Wannier Theory) and at high (Born approximation) E, is given by [28]:

$$\sigma_{MX,E} = \sigma_{MX} \ 3.86 \ [\ (E_{MX} - B_{MX})(E_{m,MX} - B_{MX})^{-1}]^{1.127} \div [0.8873 + (E_{MX} - B_{MX})(E_{m,MX} - B_{MX})^{-1}]^{2.127}. \qquad (8)$$

This model is also applicable at $E > E_m$, but is subject to the approximation of single orbital dominance. A test of the model on the σ (E) vs. E curves for Mg, Ag [16], and GaCl [25] shows very good agreement with experiment and to E > 100 eV. Thus, where E_m is reasonably well known, this model can be coupled with the MCM model – determination of σ_m to provide a complete curve of σ (E) vs. E. For known E_m , eq. (8) is estimated to yield $\sigma_{MX,E}$ values with an additional $\delta \sim 10\%$ over that of σ_m. For estimated E_m , an additional $\delta \sim 30\%$ is possible. In view of the apparent utility of this scaling approach for expanding the range of application of the MCM model to more than a single energy (E_m), the desirability of measuring E_m , where possible, is clear.

3. Results and discussion

3.1 Comparison of model with experiment

As a test of the model, and for the possible identification of anomalous or erroneous experimental molecular cross sections, we compare in Table 1 and Fig. 1 model and, to the extent possible, all known experimental values. Only σ_m comparisons are given here as most of the experimental data are at or near E_m. In the previous section (2.6) methods were given for scaling to or from other energies.

The model results were calculated using eq. (3) and the following examples illustrate the process involved. Consider SiF, where the electronegativities of Si and F indicate Si^+F^- as the likely electron configuration to be considered with the ionic MCM model. The isoelectronic M′ and X′ are then Al and Ne, respectively, from which the bracketed term of eq. (3) becomes:

$$(\sigma_{Al} B_{Al} + \sigma_{Ne} B_{Ne}).$$

The maximum ionization cross sections of Freund et al [16] and the corresponding ionization potentials are used to determine this term and hence σ_{SiF} , the maximum ionization cross section (see Table 1a). For the homonuclear case, consider C_2 as an example. According to the proposed formalism (section 2.3.2), the electronic structure is $C^{2+} :: C^{2+}$ for which M′ = Be. Hence the bracketed term becomes $(2\sigma_{Be} B_{Be})$, from which the maximum ionization cross section for C_2 is determined.

Uncertainties (δ) associated with experimental cross section data were considered in [1] for a number of the molecules included in Table 1. Reported δ values range from 10% to 100%, or more, with 20% being typical of the more accurate results [25]. For the MCM model, we estimate the σ uncertainties to be within $\delta = \pm 30\%$. Input data uncertainties to the model include (δ values in parentheses): B_{MX} (5%), $B_{M'}$ (<1%), k (<2%), $\sigma_{M'}$ (20%). In addition, for the range of E_m/B values considered here, the model approximations discussed in section 2.1 are estimated to be reliable to within δ = 20%. The overall model uncertainty estimate is supported by model-experimental comparisons for over 50 molecules where δ < 30%.

In keeping with the primary model objectives, the survey of experimental σ data is limited, in Table 1.a, to condensible inorganic species where the bonding is appreciably ionic. In Table 1.b we consider, in addition, several significantly covalent species for comparison purposes. A survey of experimental and various model results for primarily covalently bonded, gaseous species (some inorganic) has recently been made by Deutsch et al [29], and supplemented by Probst et al [30]. Before discussing the tabulated results, we reiterate the degree of independence of the model from experimental values, with the exception of the scaling factor (k) which is based on a small set of experimental values.

3.1.1 Treatment of experimental data

The following comments pertain to procedures used to obtain the experimental results of Table 1. For $NaBO_2$ and KBO_2 , the σ_e experimental values are based on model values of NaF (~ 1.0) and KF (~ 1.2) respectively. The experimental values are probably lower limits as the electron impact energy used may have been less than E_m. For C_2 , the BEB model value [32] is used as an "experimental" result. A moderately higher value ($\sigma = 3.9$) was calculated [29] using the so-called DM formalism. Similarly, for C_3F_8 [34] and SiF_4 [4, 32], the BEB model values are used as "experimental."

Where possible, or necessary, the experimental values have been scaled to an appropriate E_m for comparison with the model. This was done for the species ZrO_2 , CeO_2 , ThO_2 , ThO, NaCl, CsCl, PbS, PbSe, PbTe, LiF, BaO, in addition to S_2 , Se_2 , As_4 and Te_2 using the scaling procedures discussed in section 2.6, with preference given to that of eq. (8) where possible. Many of the experimental σ values are the result of σγ species ratio measurements, with γ ratios either estimated as an $M^{-0.5}$ or $M^{-0.4}$ dependence

or neglected. In a few instances, γ has been measured (eg. [20]) without any obvious systematic or predictable trend for high temperature molecules. For the most part, γ uncertainties are within δ limits but the rare possibility of an $\delta > 30\%$ in σ due to unmeasured or poorly estimated γ's cannot be discounted. Usually, the experimental value of σ will be too high if an unaccounted for γ–effect is present.

3.1.2 Treatment of model data for autoionization

For SiF, the autoionization-enhanced σ for Al [16] was used as the model M′ value. Similarly, for YO, the autoionized σ value for M′ = Rb [30] was used. For LaO, where M′ = Cs, the autoionization enhancement of Cs was estimated from Rb. This estimated enhancement for σ_{Cs} is also supported by the known autoionization of the isoelectronic case, Ba^+ [35]. The selected cross section agrees with one of the experimental determinations, namely that of Tate and Smith, as reported in [36]. For Se_2 , the M′ = Ge experimental value [16] was used. For As_4 , the autoionization value of σ_{Ga} [16] was used for M′ in the model. For GaCl and SnCl, the Freund et al [16] σ_{Ga} (autoionization) and σ_{Sn} (autoionization?) values are used for the covalent case. Similarly, for the ionic component of GeCl, σ_{Ga} [16] was used.

3.1.3 Partial covalent cases

A few representative cases where the bonding character is between the extreme cases of ionic or covalent are considered in Table 1.b. An average value of the two model cases gives very good agreement with experiment. We are reluctant to extend the model to cases that are even more covalent, owing to an ambiguity in assigning an appropriate M′ (or X′), and the likely significant contributions of high energy orbitals together with high E_m values (as discussed in section 2.1). A case in point is $HgBr_2$, where σ vs. α (polarizability) correlations (see section 3.3) and other considerations indicate a predominantly covalent character. High values of $\sigma \sim 20$ and $E_m \sim 70$ eV are found experimentally [37]. Additivity of the elements gives $\sigma \sim 15.4$, which is still within the $(\delta) \sim 30\%$ uncertainty for model – experimental σ comparisons. A similar value is obtained from σ vs. α relationships (section 3.3). The species In_2O and In_2S also appear to be predominantly covalent and the reported [1] In_2O/In cross section ratio (with δ of $\pm$ 50% and hence not included in Table 1) agrees with either a covalent or a partly ionic, autoionization (see section 3.2) model prediction.

3.1.4 Discussion of results

A source of potential difference between model and experiment, eg. as with VO, results from difficulty, in the latter case, in accounting for all ion contributions to σ_e. In some instances the σ_e results may be partial σ's only and hence represent a lower limit to σ - total. For SiF_3 , the model result is notably higher than experiment (Table 1). We

note that the model use of B to represent all contributing orbitals, including those with energies higher than B, could lead to too large a σ value. However, the BEB model, which includes all appropriate orbitals, leads to a similar disagreement [4]. This anomaly has been discussed in the literature in terms of a steric interference effect of each F^- restricting access by the incoming ionizing electron to the lone electron on Si^{3+} [38]. Such steric effects are not readily accounted for by this or other models except to the extent that they affect B, but even if they occur such cases appear to be rare. Also, steric effects appear to be more significant at higher E [39] and E_m for SiF_3 is uncharacteristically high considering its open-shell electron configuration.

Another case where the model is notably higher than experiment is UO_2. Perhaps a similar steric effect to that discussed for SiF_3 is the cause of the low experimental value. However, the experimental difficulty associated with accounting for fragmentation and the simultaneous presence of UO and UO_3 may also contribute to a low experimental result (see also section 3.2).

For CS (Table 1.b), the MCM ionic case ($C^{2+}S^{2-}$) somewhat fortuitously is in exact agreement with experiment. This is surprising in view of the similar electronegativities of C and S and a high degree of covalency in CS. The electron pair bond model (for : C : : S :) gives essentially the same result, whereas an average value for C_2 and S_2 is $\sigma \sim 4.5$. For As_4O_6 , an additional lower E experimental value is 10.6 at 20 eV [33]. With E-scaling, this value is consistent with the higher E value listed.

Inspection of Table 1, and the corresponding graphical representation of Fig. 1, indicates no case where model and experiment disagree to more than the $\delta = \pm 30\%$ uncertainty estimate. This is remarkable agreement as the experiments, except in a few instances, are lacking in precision and the model is greatly simplified from the usual classical approaches. These results, then, serve to provide (a) overwhelming empirical support for the reliability and general utility of the model, and (b) support for the overall reliability of the various experimental approaches and results.

Several empirical observations of σ trends [1] are also supported by the model. For the empirical ratios of partial cross sections, $\sigma_{MO}/\sigma_M \sim 0.65 \pm 0.1$, the corresponding average model value is 0.63; however the range is from 0.09 (BaO/Ba) to 0.99 (UO/U). As the model values are for total σ's, they represent an upper limit for comparison with experiment. Similarly, for the experimental ratios $\sigma_{MO2}/\sigma_{MO} \sim 0.5 \pm 0.25$, the average model value is 0.4 with a range of 0.2 to 0.9. The outliers notably have significantly different electron configurations which, as the model reveals, are a key determinant for the magnitude of σ.

3.1.5 Comparison with other models

Conceptually, one could envision possible extension of the model, eg. to include, explicitly, higher level orbitals and E/B terms. However, given the demonstrated model reliability, additional complexity does not appear warranted, even where feasible. It

appears that the use of $\sigma_{M'}$ and $\sigma_{X''}$ terms in the model adequately represents the orbital occupation and energy-dependence characteristics of the MX species being modeled. This assertion is well supported from a comparison of the MCM and BEB [4] model results for SiF_2 , and SiF_3 , where the two models give essentially the same result. For SiF, some partial improvement in agreement between the BEB model and experiment was obtained if the kinetic energy terms in the BEB model were reduced, arbitrarily, by a factor of 3 [4]. However, the contribution of autoionization (see section 3.2) seems a more likely explanation for the low BEB model σ_m value for SiF, which is based on direct ionization only. The MCM model results also compare favorably with the DM model [29, 30], eg. for BF_3 , CF_2 , CF, and C_2.

Model extension to the determination of partial ionization cross sections (σ_i) is considered impractical although, for relatively simple high temperature species, the ionic bonding concept does provide guidance to the degree of electron impact fragmentation expected [40]. For a few simple covalent species, a semiempirical model (at high E) has been used recently [41]. The most practical approach to determining σ_i appears to be the experimental determination of fragmentation pathways, coupled with the use of model σ_m.

3.2 Autoionization in molecular species

As indicated above (section 2.5), autoionization is reasonably well established as a contributing pathway to ionization for a select number of atoms. However, there appear to be no established cases for molecules in general and for ionic bonded species in particular. Application of the MCM σ model, where direct ionization atomic σ's [7] are used, provides direct ionization molecular cross sections. For cases where the model values lie well below experimental values, autoionization is reasonably indicated. A few such cases, discussed in section 3.1.2, are given in Table 1.

Where use was made of available $\sigma_{M'}$ data containing the effect of autoionization, the σ_{MX} model result usually agreed well with experiment, thereby confirming the assignment of molecular autoionization, eg. for SnCl, GaCl, GeCl, SiF, YO, and LaO. It is particularly pertinent that the BEB model result for SiF using direct ionization only [4] is significantly less than the experimental value whereas the MCM result using M′ = Al agreed with experiment. Notably, no cases of an enhanced autoionization (ie. >M′) due to molecule formation were indicated.

Another possible candidate species for autoionization is UO. However, in this case where M′ = Th, no work appears to have been done yet that would reveal autoionization in Th, although such a heavy atom is a reasonable autoionizing candidate [19]. For UO, several reasons may be offered to explain the difference between the two experimental σ values (see Table 1). First, as was pointed out by the authors of the higher value [27], the number of coexisting species and the presence of extensive electron impact fragmentation complicates the quantitative assignment of UO^+ to UO vs. UO_2 and UO_3. However, the

peaking of UO^+ ion intensity ($\sim \sigma$) at low E is pronounced and experimental error may not be the sole explanation. The most likely physical phenomenon is autoionization to an excited energy state of UO^+ above, but very near, the ionization threshold. This process could produce a strongly peaked appearance potential curve at low energies. At high energy, the direct ionization process would be more evident. Hence the lower apparent σ_{UO} value at high E most likely mainly represents the direct ionization process.

With the ionic model, the electron configuration of U^{2+} is represented by Th ~ (Rn) $7s^2\,6d^2$, modified by the field of O^{2-}. Ionization of UO would then lead to a configuration Th^+ ~ (Rn) $7s^2$ 6d, with low lying configurations of (Rn)7s $6d^2$ and (Rn)$7s^2$7p also present. A similar known autoionization case, $Ca^+ \rightarrow Ca^{2+}$ involves 4s → 4p transitions [35]. In this case, electron impact results in an electron transition to a quasi-bound state of Ca^+ above the ionization threshold. This effect in UO should be evident in an appearance potential curve of Th^+(Th). A small segment of the Th^+(Th) AP curve is known [42] near the threshold, with an apparent $E_m \sim 12$ eV, as compared with a calculated [7] direct ionization value of 31 eV. This E_m difference is consistent with autoionization. Also, the low E_m value for Th is consistent with the corresponding value for UO of ~ 8 eV. However, for the limited data available, no sharp peaking is apparent for Th^+, unlike the case for UO.

Depending on the location of M^+ energy levels that lie above B, it appears that one may find autoionization enhancement of σ over a narrow ΔE interval near B or, more typically, over a wide ΔE range at E >>B. Thus cases may occur where no enhancement is apparent at high E, eg. as with UO [43] and the σ model would then remain applicable if $E_m >> E$ for autoionization resonance.

With respect to the σ_{UO} behavior at low E, we conclude that both the experimental artifact and autoionization arguments presented here are plausible, but that further work is needed. For this reason, the higher value of σ_{UO} given in Table 1 was not included in Fig. 1 even though the data point falls within the $\delta \sim 30\%$ uncertainty limit.

The reported ratio $\sigma\gamma$ (Sc)/ $\sigma\gamma$ (Ag) = 4.17 at 25 eV [44] indicates $\sigma_{Sc} \sim 14$, vs. the direct ionization value of 9.5 [7]. However, application of this value of σ_{Sc} (ie. as M′) to the σ_{VO} model would increase the model value to well above the experimental result. This observation suggests the high σ_{Sc} value to be in error, even though Sc is an a priori candidate for autoionization.

Based on known or expected autoionization for M′, the following representative species types may be expected to show enhanced σ's due to autoionization. For each set, M′ is indicated in parentheses:

SrF , Sr_2O, (Rb); BaF, Ba_2O, ZrF_3 , ZrOCl (Cs); CF (B); SiCl (Al); GeF, AsO (Ga); SnF, SbO (In); PbCl, BiO (Tl); TiF, VF_2 , CrF_3 (Sc); ZrF, NbO, $MoCl_3$

(Y); CeF, PrO, $NdCl_3$ (La); MnF, FeO, CoF_3 (Cr); ScO, TiF_3 , (Ca^+ [37]); CeF_3 (Ba^+ [37]); ZrF_3 (Sr^+).

Based on the known autoionization of Ca^+ and Ba^+, one might anticipate similar behavior for Mg^+ and hence for AlO and SiF_3. However no evidence for autoionization was found for SiF_3 (see Table 1).

Similar examples for M_2 species include:

Si_2 (Al); As_2 (Ga); Sb_2 (In); Bi_2 (Tl); La_2 (Cs), etc.
For these candidate species, those based on M′ = B, Al, Ga, In, Tl, are expected to show an autoionization enhancement of ~37%, in slight excess of the model δ = 30% uncertainty limit. For the other cases, the difference between direct [7] and autoionization [16] $\sigma_{M'}$ is less than 20% and a similar degree of enhancement is expected for the counterpart molecular species.

For CF, the reported experimental $\sigma_m \sim 1.5$ (loc. cite [29]) and the MCM model values agree for M′ = B where the direct ionization σ_B value [7] is used. However, applying a model-predicted autoionized σ_B value [21] with the MCM model gives $\sigma_{CF} \sim 2.6$. On this basis we suggest that the σ_{CF} experimental value is too low.

In concluding these considerations of autoionization in molecular species, we reiterate the key observation that the isoelectronic atom (M′), with established autoionization cross section enhancement, provides a good representation of autoionization in MX. At the present time, no other models are able to consider autoionization in molecular species.

3.3 Model cross section – polarizability (α) relationships

Empirical relationships, with some theoretical rationale, between σ and α have often been noted in the past [45, 46], principally for covalent species. Similar underlying factors influence both σ and α, namely the presence of low lying electronic states, the spatial extension of orbitals, and the ease of electron transfer to higher states.

The general trends of α, known for a few anions and cations [47], within the periodic system and those of σ_M^+ and σ_X^-, or of σ_{MX} in the present model, are found to be similar. Table 2 shows a convincing comparison between σ and α data, particularly for the cesium and magnesium halides which were modeled (see Table 1 for CsCl, CsI) as an anion X′ case. The σ_{MX} model values for CsCl, CsBr, CsI also duplicate, exactly, the trend for α_{HX} for the corresponding hydrogen halides [45]. The close correspondence between α_X^- and model σ_{MX} is particularly striking and may be taken as verification of a direct σ vs. α relationship and of the MCM model. Values of α_X' show similar trends but are about a factor of two less than the corresponding α_X^- and cesium halide σ_{MX}

values. This latter observation is consistent with our earlier comments (section 2.2) concerning $\sigma_X^- > \sigma_X'$. It follows from the above observations that the MCM model may be used to estimate anion and cation polarizabilities.

In Table 2 we also compare known molecular α's for inorganic species [48] with the corresponding model and experimental σ's; the same general trends are found, particularly if the bond component to α can be separated from total α [49]. On the basis of the good one-to-one correlation found between σ and α, it is reasonable to suggest that the relatively high $MgBr_2$ and UF_6 experimental cross sections may be in error. Indeed, experimental difficulty with $MgBr_2$ was noted owing to the presence of oxybromide impurities. The σ vs. α relationship observed here follows that suggested earlier for covalent species [46].

3.4 Dimer cross section rules

For dimer species of the type M_2 , $(MX)_2$ etc., cross sections are usually estimated from:

$$\sigma_{M2} \sim 1.5\, \sigma_M \quad [5]$$

or

$$\sim 1.8\, (\pm 0.2)\, \sigma_M \quad [1].$$

The M_2 species considered in Table 1 indicate, however, that the model monomer to dimer factor varies significantly for different M, ie.: $C_2/C = 1.6$, $Ag_2/Ag = 1.5$, $As_4/As_2 = 1.8$, $S_2/S = 1.4$, $Se_2/Se = 1.2$, $Te_2/Te = 1.1$.

For $(MX)_2$ species, the MCM model reduces to the form:

$$\sigma_{(MX)2} = 2(B_{MX})(B_{(MX)2})^{-1}\, \sigma_{MX}.$$

Values in the range of 1.7 – 1.9 are then calculated for the monomer to dimer factor for the following alkali halides: LiCl, NaCl, KCl, and CsCl, which are somewhat higher than the literature approximation of 1.5. On this basis, reported [5, 6] partial pressures of these alkali halides could be high by about 20%.

3.5 Model comparison with additivity and consequences for thermochemical studies

A few representative cases are considered in Table 3 in order to indicate the differences between the conventional additivity and MCM models. In recent years, the likely overestimation of σ's using the additivity model has been recognized and an arbitrary 25% or other empirically based reduction has sometimes been made (see discussion in [1]). However, as shown in Table 3, reductions of about 1000% may sometimes be necessary, particularly for closed shell electron configurations. For open shell cases, the errors are not so egregious, typically less than 100%. That such

differences can be expected is readily apparent from inspection of the periodic nature of σ_M and B_M and the sharp differences present between adjacent elements, corresponding to $M \rightarrow M^+$ or $X \rightarrow X^-$, for instance.

The authors of the comprehensive thermochemical database IVTANTERMO [5] have allowed for molecular σ uncertainties of 150% in their error assessments. They also follow the dimer/monomer ~ 1.5 σ rule. A σ uncertainty of 150% typically leads to an uncertainty in high temperature enthalpies of ~ 8 k Joule $mole^{-1}$, depending on temperature, and can be the main source of data uncertainty. As we have shown, even this seemingly conservative σ uncertainty estimate can be low by an additional factor of six.

In view of the possibility of large errors associated with ionization cross section estimations, one might expect to find literature examples where, eg. Second and Third law – based enthalpies, or D^o_{MX} obtained from mass spectrometric equilibria vs. spectroscopic, photodissociation etc., disagree beyond the expected experimental uncertainties. Without resorting to a systematic search for such cases, several representative examples are considered as follows.

The enthalpy of formation of SiF_2 is based on measured enthalpy changes (ΔH) for reactions such as

$$2CaF + Si = 2Ca + SiF_2.$$

In this particular case, the Second and Third law ΔH's differ by about 40 k Joule $mole^{-1}$ [50]. For the Third law determination, the additivity σ model was used. Application of the MCM model indicates that this procedure overestimates the reaction equilibrium constant by at least an order-of-magnitude, which corresponds to 20 k Joule $mole^{-1}$. With this correction, the Second and Third law ΔH's differ by a more acceptable 20 k Joule $mole^{-1}$.

Similarly, for the well-studied case of AlO, original differences between D^o_{AlO} from MS vs. spectroscopic methods [5, 6] can be explained through use of lower σ_{AlO} values predicted from the present model.

An example of application of a modified additivity model is the PN system [51]. For PN, additivity, modified additivity, and the MCM model lead to the following σ values: 6.0, 7.2, and 3.3 respectively. Hence, in this case, the reported partial pressure (p) of PN, resulting from this σ analysis, is likely to be too low by a factor of two (as $p \sim \sigma^{-1}$).

A further example, where the Gryzinski model was used to calculate σ_{LiF} and hence LiF partial pressures, is as follows [52]. The authors used the ratio σ_{LiF}/σ_{Ag} =

0.61, as compared with the present value of 0.2 (from Table 1). Hence their LiF partial pressures are too low by a factor of three. A comparison of their pressures with those of JANAF [6] indicates the latter to be a factor of 2.5 x greater, which is consistent with the use of too high a σ_{LiF} value in [52].

Other examples of excessively low mass spectrometrically determined partial pressures (by an order of magnitude) were noted more than thirty years ago for species such as PtO_2 and RuO_3 [53]. One of the explanations offered by the authors was the possible use of estimated cross sections that were too high. Application of the present model to their data does explain, at least in part, the observed discrepancies between the mass spectrometric and transpiration vapor pressures.

For other cases, where the bonding is significantly covalent and/or the electron configuration is open-shell, earlier estimates are not too different from the MCM model values and thermodynamic data inconsistencies are not as apparent. For instance good Second-Third law accord is found for D^{o}_{LaSe} [54].

From these few examples it is apparent that past practice in estimating ionization cross sections can lead to significant errors in thermochemical data. However, as has been discussed in detail elsewhere [1], with the use of appropriate experimental and data analysis procedures, such errors can often be avoided or their presence at least revealed. For those cases where reliance on cross sections is unavoidable, application of the present model should markedly reduce the data uncertainties.

4. Summary

In summary, the following procedure is recommended in applying the MCM cross section model. First, identify the likely ionizing electron character (bonding, non-bonding, cation-like...) based on the ionization potential change resulting from molecule formation, or the change in bond energy on ionization. Second, identify from common valence considerations whether the constituent cations and anions have a closed or open shell electron – complement. Third, identify if the molecule can be expected to have some covalent character, or if its many atom complement (typically > 3 atoms) would favor significant electron delocalization. This criterion essentially represents the degree to which the molecule can be expected to depart from the ideal case of complete ionic bonding. From these three steps, it should be possible to attribute either anion, or anion together with cation, as contributors to ionization. Then use the isoelectronic counterpart atoms to simulate the cross sections of the component ions. This information, together with a knowledge of the molecule ionization potential, is sufficient to allow for prediction of ionization cross sections for virtually any high temperature species or other inorganic molecule.

The accuracy of the model predictions appears comparable with or, in some instances, better than that of experimental methods. A least squares difference of only 2% is found from a comparison between the model and experimental values for fifty-one molecules. For an individual species, the main source of model uncertainty appears to

arise from the cross sections of the isoelectronic atoms. For the most part, the calculated direct ionization values of Mann [7] and, more recently, of others [22, 55], appear sufficiently accurate for use with the model. For the few cases where an unknown autoionization contribution may be present, the model values could be low but still within the assigned 30% uncertainty limit.

Acknowledgements

Discussions with Dr. Yong-Ki Kim on the BEB model and autoionization of Al, Ga, and In are acknowledged, in addition to general discussions with colleagues Drs. David W. Bonnell, Jean Drowart, and Christian Chatillon on cross sections and high temperature mass spectrometry.

References

[1] J. Drowart, C. Chatillon, J.W. Hastie, and D.W. Bonnell. "Determination of Thermodynamic Properties for Condensed Phases and Gases with the Mass Spectrometric Knudsen Cell and Vapor Transport Methods: Accuracy, Precision, and the Influence of Ionization Cross Sections," to be published, Pure Appl. Chem. (2001).

[2] K.S. Krasnov, N.V. Karaseva, Opt. and Specty., 19 (1965) 14; J.L. Margrave, J. Phys. Chem. 58 (1954) 258. These are representative works, amongst numerous others.

[3] J.W. Hastie, J.L. Margrave, Fluorine Chem. Rev. 2 (1968) 77.

[4] W. Hwang, Y-K Kim, M.E. Rudd, J. Chem. Phys. 104 (1996) 22.

[5] L.V. Gurvich, I.V. Veyts, C.B. Alcock, Thermodynamic Properties of Individual Substances, 4th Ed., Vols. 1 – 3. Hemisphere Pub. Corp., N.Y., 1989.

[6] M. Chase, Jr., NIST – JANAF Thermochemical Tables, 4th Ed., J. Phys. Chem. Ref. Data Monograph 9, NIST, Gaithersburg, MD, 1998.

[7] J.B. Mann, In Recent Developments in Mass Spectroscopy, Proc. Conf. Mass Spectroscopy, Tokyo (K. Ogata, T. Hayakawa, Eds.), University Park Press, Baltimore, MD, 1970, p. 814; also J. Chem. Phys. 46 (1967) 1646; more recently a similar formalism (known as DM) has been used, with empirical input, for gaseous molecular species [29].

[8] M. Gryzinski, Phys. Rev. A 2 (1965) 336.

[9] B. Peart, S.O. Martin, K.T. Dolder, "Recent Measurements of Cross Sections for the Ionization of Ions by Electron Impact," in Sixth Intl. Conf. Phys. and Electron and Atomic Collisions, 1969, p.1.

[10] R. Rich, Periodic Correlations, W.A. Benjamin, Inc., N.Y., 1965.

[11] M.A. Lennon, K.L. Bell, H.B. Gilbody, J.G. Hughes, A.E. Kingston, M.J. Murray, F.J. Smith, J. Phys. Chem. Ref. Data 17 (1988) 1285.

[12] T.R. Hayes, R.C. Wetzel, F.A. Baiocchi, R.S. Freund, J. Chem. Phys. 88 (1988) 823.

[13] R.J. Shul, T.R. Hayes, R.C. Wetzel, F.A. Baiocchi, R.S. Freund, J. Chem. Phys. 89 (1988) 4042.

[14] T.R. Hayes, R.J. Shul, F.A. Baiocchi, R.C. Wetzel, R.S. Freund, J. Chem. Phys. 89 (1988) 4035.

[15] J.W. Hastie, J.L. Margrave, High Temp. Science 1 (1969) 481.

[16] R.S. Freund, R.C. Wetzel, R.J. Shul, T.R. Hayes, Phys. Rev. A 41 (1990) 3575.

[17] J.W. Hastie, J.L. Margrave, J. Phys. Chem. 73 (1969) 1105.

[18] Y.-K. Kim, J. Migdalek, W. Siegel, J. Bieron, Phys. Rev. A 57 (1998) 246.

[19] E.W. McDaniel, Atomic Collisions, Wiley and Sons, N.Y., 1989, p. 392.

[20] R.T. Meyer, A.W. Lynch, High Temp. Science 5 (1973) 192.

[21] Y.-K. Kim, P.M. Stone, "Ionization of Boron, Aluminum, Gallium and Indium by Electron Impact," in press, Phys. Rev. A (2001).

[22] Y.-K. Kim, M.E. Rudd, Phys. Rev. A 50 (1994) 3954.

[23] R.H.G. Reid, Photon and Electron Collisions with Atoms and Molecules, Ed. P.G. Burke, C.J. Joachain, Plenum, N.Y., 1997, p. 37.

[24] D.W. Bonnell, J.W. Hastie, K.F. Zmbov, High Temp. High Press. 20 (1988) 251.

[25] R.J. Shul, R.S. Freund, R.C. Wetzel, Phys. Rev. A 41 (1990) 5856.

[26] J.W. Hastie, Pure Appl. Chem. 56 (1984) 1583.

[27] P.E. Blackburn, P.M. Danielson, J. Chem. Phys. 56 (1972) 6156.

[28] J.M. Rost, T. Pattard, Phys. Rev. A 55 (1997) R5 – R7.

[29] H. Deutsch, K. Becker, S. Matt, T.D. Mark, Int. J. Mass Spectr. 197 (2000) 37.

[30] M. Probst, H. Deutsch, K. Becker, T.D. Mark, Int. J. Mass Spectr. 206 (2001) 13.

[31] K.J. Nygaard, Y.B. Hahn, J. Chem. Phys. 58 (1973) 349.

[32] Y.-K. Kim, private communication of unpublished BEB model result, NIST, 2001; result of [29] also from a model.

[33] J.W. Hastie, unpublished observation, NIST, 2001.

[34] H. Nishimura, W.M. Huo, M.A. Ali, Y.-K. Kim, J. Chem. Phys. 110 (1999) 3811.

[35] D.C. Griffin, M.S. Pindzola, C. Bottcher, J. Phys.. B. At. Mol. Phys. 17 (1984) 3183.

[36] R.H. McFarland, Phys. Rev. 159 (1967) 20.

[37] W.J. Wiegand, L.R. Boedecker, Appl. Phys. Lett. 40 (1982) 225.

[38] M. Bobeldikh, W.J. Van der Zande, P.G. Kistemaker, Chem. Phys. 179 (1994) 125.

[39] C. Vallance, S.A. Harris, J.E. Hudson, P.W. Harland, J. Phys. B: At. Mol. Opt. Phys. 30 (1997) 2465.

[40] J.W. Hastie, J.L. Margrave, High Temp. Sci. 1 (1969) 48.

[41] S. Pal, S. Prakash, S. Kumar, Int. J. Mass Spec. 184 (1999) 201.

[42] R.J. Ackerman, E.G. Rauh, High Temp. Science 5 (1973) 463.

[43] A. Pattoret, J. Drowart, S. Smoes, Trans. Faraday Soc. 65 (1969) 98. See also [1].

[44] L.L. Ames, P.N. Walsh, D. White, J. Phys. Chem. 71 (1967) 2707.

[45] P.W. Harland, C. Vallance, Int. J. Mass Spec. Ion Proc. 171 (1997) 173.

[46] F.W. Lampe, J.L. Franklin, F.H. Field, J. Amer. Chem. Soc. 79 (1957) 6129.

[47] M.J. Sienko, R.A. Plane, Physical Inorganic Chemistry, W.A. Benjamin Inc., N.Y., 1963.

[48] CRC Handbook of Chemistry and Physics, 79th Ed., CRC Press, N.Y., 1998.

[49] R. Kremens, B. Bederson, B. Jaduszliwer, J. Stockdale, A. Tino, J. Chem. Phys. 81 (1984) 1676.

[50] T.C. Ehlert, J.L. Margrave, J. Chem. Phys. 41 (1964) 1069.

[51] M. Guido, G. Gigli, High Temp. Science 7 (1975) 122.

[52] M. Yamawacki, M. Hirai, M. Yasumoto, M. Kanno, J. Nucl. Sci. Tech. 19 (1982) 563.

[53] J.H. Norman, H.G. Staley, W.E. Bell, Advan. Chem. Series 72 (1968) 101.

[54] R.Y. Ni, P.G. Wahlbeck, High Temp. Science 4 (1972) 326.

[55] H. Deutsch, K. Becker, T.D. Mark, Int. J. Mass Spec. Ion Proc. 151 (1995) 135.

Table 1.a - Molecular Species Model (σ_m) and Experimental (σ_e) Maximum Ionization Cross Sections, Ionization Potentials (B) and Maximum Energies (E_m)

Species	Model [d] σ_m (10^{-20} m^2)	Experimental σ_e (10^{-20} m^2)	Ionization Potential B, eV	Max Energy [a] E_m, eV
		Closed Shell		
LiF	0.9	1.0 [24] b	11.3 c	55 [52]
Li_2O	1.7	2.0 [1]	6.2 c	~70
NaCl	2.3	2.4 [26,33]	9.1 [3]	~50
$NaBO_2$	2.3	1.9 [1]	9.2 [1]	~80
KBO_2	2.5	1.7 [1]	8.6 [1]	~70
CsCl	3.5	3.5 [26,33]	7.8 c	~50
CsI	7.1	8.0 e	6.5 c	~50
BaO	1.6	1.8 f	6.9 c	50 f
TiO_2	2.3	2.6 [1]	9.5 c	50 v
ZrO_2	2.3	2.8 g	9.5 c	25 g
CeO_2	2.2	2.0 h	9.7 c	~25 o
ThO_2	2.5	3.2 [42]	8.7	~25 o
UO_3	3.0	2.5 [27]	10.6 c	25 i
W_2O_6	13.4	11.4 [1]	12.2 c	~70
WF_6	10.0	9.5 [32]	~ 13	~70
		Open Shell		
BS_2	6.4	6.9 [1]	~8.5	~60
SiF	6.5	6.4 [12] t	7.3 [12]	30
SiF_2	4.8	4.2 [13] u	11.2 [13]	80
SiF_3	4.8	3.4 [14]	9.2 [14]	90
SiO	3.4	3.1 [1]	10.8 c,n	~30
TiO	7.5	6.8 j	6.7 c	30 v
VO	6.5	4.7 [1]	7.4 [1]	~30
YO	7.9	8.1 [1,44]	5.9 [1]	~20 m
ZrO	8.6	(8.6) g	6.5 c	~25 g
LaO	8.6	9.7 [1,44]	4.9 [1]	~20
CeO	12.8	11.0 h	5.2 [1]	11 h
ThO	11.1	11.0 [1,42]	6.1 [1]	16 [42]
UO	15.7	14.1 [1] 17.0 [27]	4.7 [27] p	~50 [43] 8 [27]
UO_2	14.3	11.6 [27]	5.5 [27]	18 [27]
VO_2	2.0	1.5 [1]	9.6 [1]	~20
PbS	8.0	6.6 [1]	8.6 [1]	~50
PbSe	9.0	8.2 [1]	8.4 [1]	~50
PbTe	10.5	11.5 [1]	8.3 [1]	~50
GdS	11.4	10.8 [1]	6.9 [1]	~20
US	16.0	17.2 [1] q	5.6 c	~30
C_2	3.4	3.2 [32] 4.0 [29]	10.9 c	~30
S_2	7.3	7.0 [1] k	9.4 c	~40
Se_2	8.2	7.9 [1] w	8.9 [1]	~40
Te_2	10.6	10 [1]	8.3 [1]	~40
Ag_2	7.8	7.5 [1]	7.3 c	~30
As_4	13.8	12.9 [1]	9.9 c	~50

Table 1.b - Heteroatom Cases With Significant (~50%) Covalency

Species	Model			Experimental	B	E_m
	Ionic	Covalent (additive)	Average			
Closed Shell						
HCl	2.0	3.6	2.8	2.3 [26] 2.7 l	12.7 c	~60
SiF_4	4.1	9.3	6.7	5.5 [32]	~13	100
C_3F_8	7.0	14,0	10.5	12.5 [34]	13.7 c	100
$TiCl_4$	11.7	22.3	17.0	15 r	11.7	30-100
UF_6	8.0	22.0	15.0	18 s	14	~80
Open Shell						
GaCl	5.4	12.6	9.0	9.1 [25]	10.1 [25]	40
GeCl	8.6	9.1	8.8	11 [25]	7.2 [25]	50
SnCl	10.4	13.7	12.0	11.7 [25]	6.8 [25]	35
CS	4.0	5.9	5.0	4.0 k	11.3 k	80
As_4O_6	18.1	27.8	23.0	23.0 [33]	9.5 [26]	~30

Table 1 Footnotes, References:

a. Estimated (~) values are based on analogy with similar species or on the corresponding values for M′ or X′ atoms, which probably provides an upper limit.

b. References, cited in main text, indicated in parentheses.

c. R.D. Levin, S.G. Lias, Ionization Potential and Appearance Potential Measurements, 1971 – 1981, NSRDS – NBS (NIST) 71 , 1982. J.G. Dillard, K. Draxl, J.L. Franklin, F.H. Field, J.T. Herron, H.H. Rosenstock, Ionization Potentials, Appearance Potentials, and Heats of Formation of Gaseous Positive Ions, NSRDS – NBS (NIST) 26 , 1969.

d. Atomic B values used in the model, available from various reference sources, eg. [48].

e. L.N. Gorokhov, N.E. Khandamirova, Advan. Mass Spec. B , Wiley and Sons, N.Y., 1985, p.1031.

f. J.W. Hastie, D.W. Bonnell, P.K. Schenck, Pure Appl. Chem. 72 (2000) 2111.

g. R.J. Ackerman, E.G. Rauh, C.A. Alexander, High Temp. Science, 7 (1975) 304; σ ratio ZrO/ZrO_2 given.

h. R.J. Ackerman, E. G. Rauh, J. Chem. Thermodyn. 3 (1971) 609.

i. Low value [27].

j. R.I. Sheldon, P.W. Gilles, in Characterization of High Temperature Vapors and Gases, NBS (NIST) SP 561, Ed. J.W. Hastie, U.S. Govt. Clearinghouse, 1979, p. 231.

k. R.S. Freund, R.C. Wetzel, R.J. Shul, Phys. Rev. A 41 (1990) 5861; a value of 5.7 is given as a partial σ for the parent ion.

l. From σ vs. α relationship.

m. Rb has two peaks at 10 and 40 eV [31].

n. An alternate B ~ 11.6 yields $\sigma_m \sim 3.1$; for B see D.L. Hildenbrand, Int. J. Mass Spectr. 197 (2000) 237.

o. Estimated from ZrO_2 E_m and periodic trends.

p. An alternate, probably more accurate value is 5.6, from G. Rauh, R.J. Ackerman, J. Chem. Phys. 60 (1974) 1396. However, we used the value of [27] to maintain a self consistent comparison with σ_e [27].

q. An alternate value of 13.7 is derived from the data of E.D. Cater, E.G. Rauh, R.J. Thorn, J. Chem. Phys. 44 (1966) 3106.

r. Cited in [29]; also DM model [29] gives $\sigma_m = 16.3$.

s. Cited in [40].

t. For the analogous species CF, $\sigma_m = 2.3$ (MCM model, σ_B auto [21]), or 2.5 (DM model [29]).

u. For the analogous species CF_2, $\sigma_m = 3.5$ (MCM model), or 3.1 (DM model [29]).

v. S. Banon, C. Chatillon, M. Allibert, High Temp. Sci. 15 (1982) 17.

w. σ_e scaled from 14 eV; an alternate σ_e value in [1] of 13.8 is considered an experimental outlier.

Table 2

Cross Section – Polarizability (α) Comparisons

Species	σ_{MX} model (10^{-20} m^2)	σ_{MX} exper. (10^{-20} m^2)	α_X^- [47] (10^{-30} m^2)	α_X' [48] (10^{-30} m^2)
CsF	1.1	–	1.0	0.4 (Ne)
CsCl	3.5	3.7	3.6	1.6 (Ar)
CsBr	4.6	–	4.8	2.5 (Kr)
CsI	7.1	8	7.1	4.0 (Xe)
			1.6 α_X^-	
MgF_2 a	1.6	(1.6) b	1.6	
$MgCl_2$	4.9	3.8	5.8	
$MgBr_2$	6.6	9.0	7.7	
MgI_2	9.3	10.4	11.4	
			α_{MX} [48]	
BF_3	4.3	3.6 c	3.3	
SiF_4	6.5	6.0 d	5.4	
SeF_6	8.7	---	7.3	
UF_6	15	18 e	12.5	
$AsCl_3$	12.7	---	14.9	
CS_2	7.6	---	8.7	

Footnotes:

a. B's, 13.5, 11.1, 10.6, 10.0 eV, from fluoride to iodide.

b. Experimental values, referenced to MgF_2 , measured by J. Berkowitz, J.R. Marquart, J. Chem. Phys. 37 (1962) 1853. These values are not included in Table 1 as they are not absolute measurements.

c. DM model [30].

d. BEB model [32].

e. Cited in [45].

Table 3

Cross Section Comparison for MCM and Additivity Models (units 10^{-20} m^2)

Species	MCM Model	Additivity
closed shell		
BaO	1.6	18.6
CsI	7.1	17.6
CsF	1.2	11.8
CeO_2	2.2	18.5
SrI	3.2	19.7
Li_2O	1.7	7.9
open shell		
As_4	13.8	20.0
As_4O_6	18.1	27.8
Se_2	6.1	10.0
TiF	6.8	9.7
Cs_2Te_2	38.3	40.2

Caption

Fig. 1. Comparison of model (σ_m) and experimental (σ_e) cross sections; solid curve represents an exact correspondence line for σ_m and σ_e which is virtually indistinguishable from a least squares fit; broken curves indicate uncertainty limits (δ) of $\pm$ 30%; least squares fit has a 0.95 coefficient of determination and the slope leads to $k = 0.62 \pm 0.01$, in agreement with the value based on four selected reference species (see text, section 2.1).

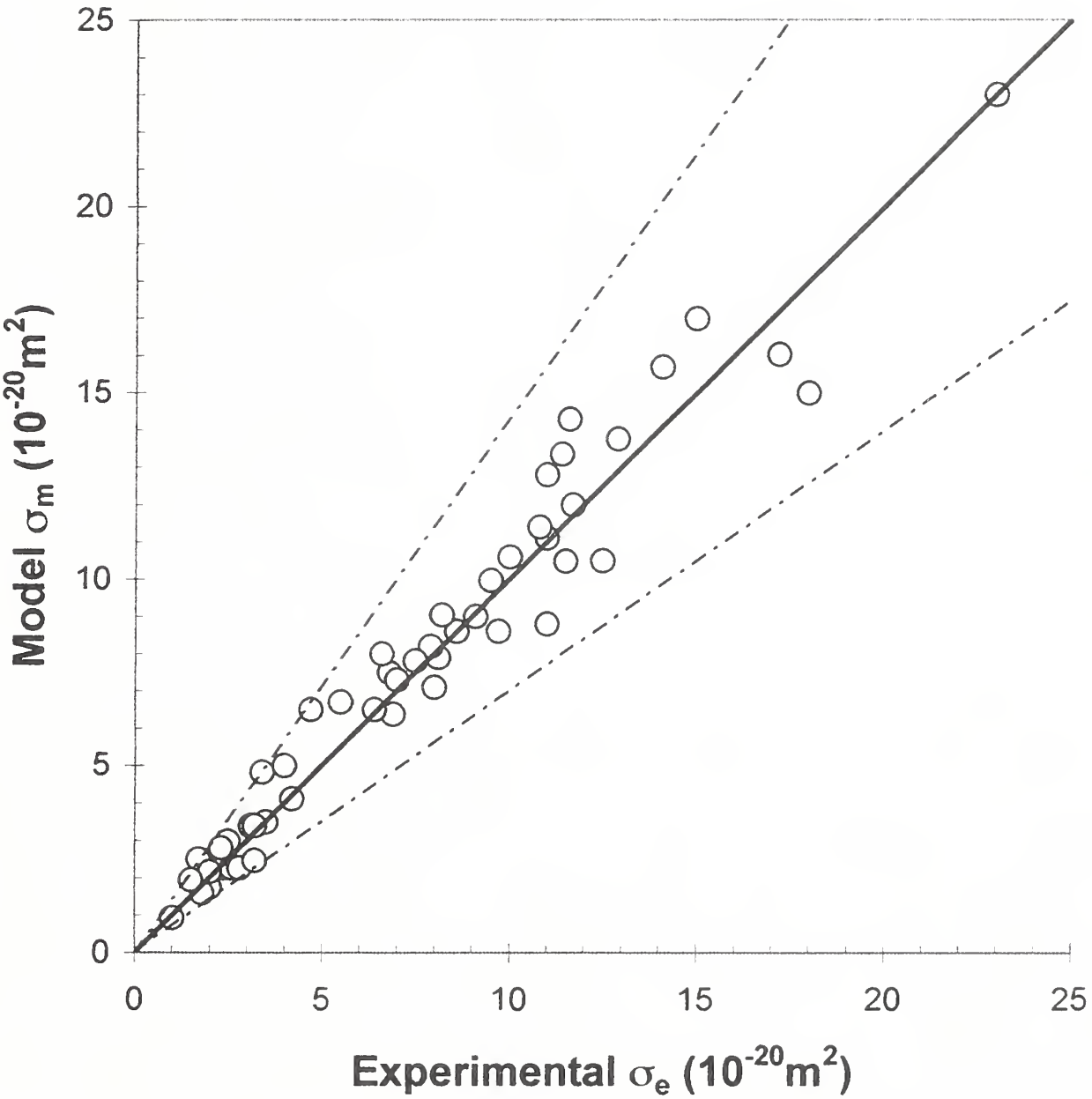
25
20
15
10
5
0
0
5
10
15
20
25
Model σ_m ($10^{-20}m^2$)
Experimental σ_e ($10^{-20}m^2$)